Available online at www.sciencedirect.com
SCIENCE DIRECT
Polymer 47 (2006) 5754–5761
polymer
www.elsevier.com/locate/polymer

Flexible, low-density polymer crosslinked silica aerogels

Lynn A. Capadona, Mary Ann B. Meador*, Antonella Alunni[1], Eve F. Fabrizio[2], Plousia Vassilaras[1], Nicholas Leventis[3]

NASA Glenn Research Center, 21000 Brookpark Road, Cleveland, OH 44135, United States

Received 3 March 2006; received in revised form 22 May 2006; accepted 29 May 2006
Available online 30 June 2006

Abstract

Polymerization of a di-isocyanate with the amine-modified surface of a sol–gel derived mesoporous silica network crosslinks the nanoparticles of the silica skeleton, and reinforces the otherwise fragile framework. Systematically adjusting the processing variables affecting density produce aerogels whose macroscopic properties could be controlled, and are attributed to changing nanoscale morphology. Aerogels crosslinked using the smallest amount of silica studied exhibit as much as a 40-fold increase in strength over the corresponding non-crosslinked framework, and are flexible.

Keywords: Polymer crosslinked aerogels; Mesoporous; Di-isocyanates

1. Introduction

Because of their low density and high mesoporosity, sol–gel derived silica aerogels are attractive candidates for many unique thermal, optical, catalytic, and chemical applications [1–3]. However, their inherent fragility and environmental sensitivity have restricted the use of monolithic aerogels to, for example, extreme applications such as insulating the batteries on the Mars Sojourner Rover where weight is at a premium and the temperature is −40 °C [4]. Future space exploration missions as well as advanced aeropropulsion systems demand lighter weight, robust, dual purpose materials for insulation, radiation protection and/or structural elements of habitats, rovers, astronaut suits, and cryotanks. Reducing fragility by crosslinking the mesoporous silica structure of an aerogel with a polymer [5–7] has the potential to foster their use as lightweight structural and insulating materials critical in aeronautics, space and commercial applications.

The mesoporous structure of silica aerogels results from a sol–gel process using tetramethoxysilane (TMOS) and a base catalyst followed by supercritical fluid extraction [4]. The mesoporous structure consists of fully dense 1–2 nm amorphous silica particles which assemble into ball-like secondary particles (5–10 nm). These secondary particles connect together through neck regions fashioned by dissolution and re-precipitation of the silica gel during aging, forming a pearl necklace-like structure containing large voids [8]. Such empty space between entangled nanoparticle strands is responsible for the low-density and low thermal conductivity of the aerogels [9,10]. When stress incident on the material causes failure, fracture occurs at the interface of secondary particles (necks), while primary particles remain intact [11]. The incorporation of a nanocast polymer coating covalently bonded to the surface of the silica framework before supercritical drying provides reinforcement by widening the interparticle necks while minimally reducing porosity [12].

We have previously reported crosslinking with isocyanate-derived chemistry utilizing surface silanols, which comprise reaction sites for the di-isocyanate [5,7]. Polymerization of

* Corresponding author. Tel.: +1 216 433 3221; fax: +1 216 977 7132.
E-mail address: maryann.meador@nasa.gov (M.A.B. Meador).
[1] NASA Undergraduate Summer Research Program.
[2] Employed by the Ohio Aerospace Institute.
[3] Present address: Department of Chemistry, University of Missouri-Rolla, Rolla, MO 65409, United States.

0032-3861/$ - see front matter © 2006 Elsevier Ltd. All rights reserved.
doi:10.1016/j.polymer.2006.05.073

the di-isocyanate oligomers, however, is not only dependent on surface –OH reactivity but also in fact builds on amines generated *in situ* when water adsorbed on the mesoporous surfaces reacts with the isocyanate moieties [7]. To create additional reactive sites and further increase strength without perhaps the addition of more weight, we have modified the underlying aerogel to include amine functionality by co-polymerization of TMOS with aminopropyltriethoxy silane (APTES) as previously reported for use with epoxy crosslinkers [6] and more recently with isocyanates [12]. For steric reasons and since hydrolysis of APTES is slower than hydrolysis of TMOS [13], the amine functionality is mostly positioned on the surface of the secondary particles where it is readily available for crosslinking [14]. Through reaction with amines, we expect a conformal polymer coating to be attached to the surface through urea linkages as shown in Scheme 1.

We have previously explored di-isocyanate crosslinked aerogels with density ranges of 0.2–0.5 g/cm^3 and have shown that these materials have very high specific strength compared to native (non-crosslinked) aerogels with a similar silica framework [7,12]. However, aerogels have been reported with densities as low as 0.003 g/cm^3 [15]. These extremely low-density materials have extraordinary insulating properties but their fragility limits their utility. Herein, we report a study centered on the improvements in mechanical properties obtained when building polymer crosslinking on a lower density silica framework.

2. Experimental section

2.1. Materials

Raw materials tetramethoxysilane (TMOS), 3-aminopropyl triethoxysilane (APTES), and high-purity acetonitrile (CH_3CN) were purchased from Sigma–Aldrich and used as received. Deionized water was obtained from a Milli-Q water purification system (Millipore). The di-isocyanate crosslinker Desmodur N3200 (average molecular weight 500) was obtained by the courtesy of Bayer Corporation and also used as received. For ease of study, the sols were poured into 5 mL polypropylene molds (Wheaton polypropylene omni-vials). Liquid carbon dioxide and siphon tube for supercritical fluid extraction were purchased and used as received from Linde Gas, Independence, OH.

2.2. Methods

2.2.1. Preparation

Using a systematic approach, the concentration of the co-polymerized silanes in the starting gel, the concentration of di-isocyanate the gels are exposed to, and the reaction temperature were varied as shown in Table 1. Wet gels incorporating 25% v/v APTES in TMOS were prepared as previously described, utilizing the amount of total silane as specified in Table 1, noting that the use of amine-rich APTES eliminates the need for additional base catalysis [6]. For all runs in the table, two separate vials were prepared: one containing the silanes in solvent, the other containing necessary water for gel hydrolysis, also in solvent. In this study, the water/solvent vial was held constant (9 mL solvent: 3 mL water) while the silane/solvent vial was varied to obtain the volume concentrations reported in Table 1. In run 1, 2.9 mL of TMOS was combined with 0.975 mL of APTES in 9 mL of acetonitrile to achieve a 30% v/v solution. Once formed, the gels were extracted from their molds and washed four times in 24-h intervals to remove residual water. To crosslink with isocyanate, typical 1 cm diameter × 4.5 cm length wet gels were placed in ~20 mL of a di-isocyanate (Desmodur N3200, a 1,6-hexamethylene di-isocyanate-based oligomer) bath of varying concentrations (as shown in Table 1) and were allowed to equilibrate until no visible concentration gradients were observed with agitation (usually 24 h). Afterwards, the monomer solution was decanted, replaced with fresh acetonitrile, and allowed to react for 72 h either at room temperature or in a 71 °C oven. At the end of the period, oven-cured gels were cooled to room temperature, and the solvent was replaced four times in 24-h intervals to remove any unreacted monomer from the mesopores of the wet gels. The solvent was removed from the gels using supercritical fluid extraction with CO_2 (Applied

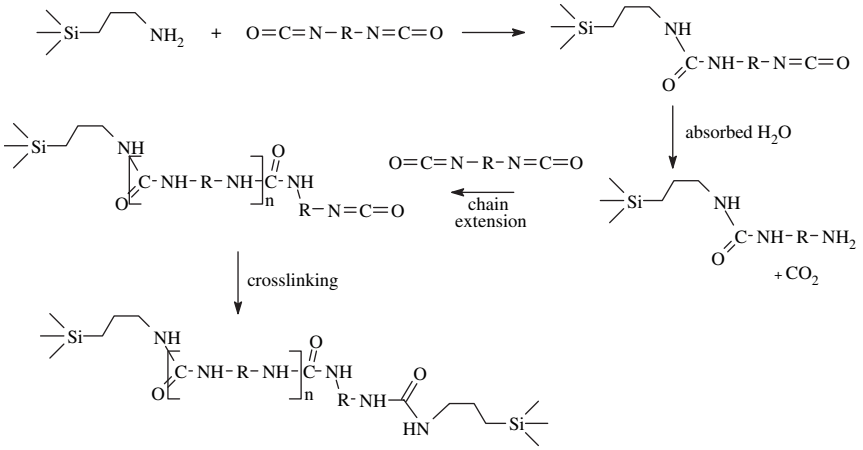

Scheme 1. Reaction scheme for amine-modified aerogel crosslinking with di-isocyanates.

Table 1
Summary of design variables and resulting properties of di-isocyanate crosslinked aerogels

Run	Total silane (% v/v in CH_3CN)	Di-isocyanate conc. (w/w in CH_3CN)	Crosslink temp. (°C)	Bulk density (g/cm^3)	Stress at failure ($Pa \times 10^4$ Pa)	Flexural modulus (MPa)	Average diameter (cm)
1	30.0	0.0	25	0.136	1.32	6.91	0.77
2	30.0	13	25	0.312	46.7	15.1	0.92
3	30.0	6.8	25	0.270	25.3	11.2	0.93
4	30.0	2.3	25	0.225	8.66	8.97	0.90
5	30.0	13	71	0.449	159	46.7	0.87
6	30.0	6.8	71	0.351	50.3	25.4	0.87
7	30.0	2.3	71	0.283	38.0	15.8	0.87
8	17.6	0.0	25	0.083	2.45	2.61	0.74
9	17.6	13	25	0.190	7.95	4.58	0.90
10	17.6	6.8	25	0.179	7.54	4.27	0.89
11	17.6	2.3	25	0.161	5.56	3.86	0.88
12	17.6	13	71	0.347	51.5	28.8	0.82
13	17.6	6.8	71	0.316	40.0	25.3	0.79
14	17.6	2.3	71	0.234	14.4	10.7	0.80
15	7.16	0.0	25	0.0420	0.667	1.01	0.76
16	7.16	13	25	0.0900	8.29	0.661	0.85
17	7.16	6.8	25	0.0830	6.92	0.437	0.84
18	7.16	2.3	25	0.0750	5.71	0.414	0.82
19	7.16	13	71	0.155	7.74	3.44	0.81
20	7.16	6.8	71	0.143	8.54	3.69	0.84
21	7.16	2.3	71	0.106	6.37	1.19	0.80
22	4.10	0.0	25	0.0260	0.0906	0.103	0.82
23	4.10	13	25	0.0430	2.22	0.123	0.79
24	4.10	6.8	25	0.0380	1.68	0.104	0.86
25	4.10	2.3	25	0.0360	1.21	0.0970	0.76
26	4.10	13	71	0.0720	3.40	0.357	0.78
27	4.10	6.8	71	0.0590	2.75	0.258	0.86
28	4.10	2.3	71	0.0570	2.11	0.213	0.84
29	30.0	13	25	0.207	147	5.25	0.93
30	7.16	2.3	25	0.0460	3.44	0.140	0.93

Separations, 1 L autoclave chamber) to produce the corresponding polymer crosslinked aerogel monoliths.

2.2.2. Characterization

Solid ^{13}C NMR spectra were obtained on a Bruker Avance 300 Spectrometer, using cross-polarization and magic-angle spinning at 7 kHz. The solid ^{13}C NMR spectra were externally referenced to the carbonyl of glycine (176.1 ppm relative to tetramethylsilane, TMS). Samples for SEM were coated with gold and microscopy was conducted with a Hitachi S-4700 field-emission microscope. For nitrogen-adsorption porosimetry, samples were outgassed at 80 °C for 24 h under vacuum and studies were conducted with an ASAP 2000 Surface Area/Pore Distribution analyzer (Micromeritics Instrument Corp.). Skeletal density measurements were made using a helium pycnometer (Accupyc 1330, Micromeritics Instrument Corp.) after being outgassed also at 80 °C for 24 h.

Three-point flexural bending tests were performed according to ASTM D790, Procedure A (Flexural Properties of Unreinforced and Reinforced Plastics and Electrical Insulating Materials), using an Instron 4469 universal testing machine frame with a 2 kN load cell (Instron part number 2525-818) and a three-point bend fixture, with 0.9 in. span and 25 mm roller diameter (Instron part number 2810-182). Typical samples were cylindrical, $\sim$1 cm in diameter and $\sim$4 cm in length. The crosshead speed was set at 0.04 in min^{-1}. Three samples were tested for each composition and the average of the three values is presented in Table 1.

2.2.3. Statistical analysis

Experimental design and analysis were carried out using the RS/Series for Windows, including RS/1 Version 6.01, and RS/Discover and RS/Explore Release 4.1, available from Domain Manufacturing Corporation, Burlington, MA.

3. Results and discussion

Twenty-eight different aerogel monoliths plus two repeats were prepared as summarized in Table 1. In these experiments, three preparation conditions have been systematically varied: silane concentration (s) at four different levels, di-isocyanate concentration (d) also at four levels and polymerization temperature (t) at two levels. The initial silane concentration (total APTES plus TMOS in a 1–3 v/v ratio) which was varied from 4.1% to 30% by volume in acetonitrile (CH_3CN) should determine the density of underlying silica aerogel, while the amount of di-isocyanate in the crosslinking solution ranging from 0% w/w to 13% w/w in CH_3CN and the cure temperature should determine the degree of crosslinking. The maximum stress at failure and flexural modulus were measured for each of the monoliths using a three-point flexural bending test [16], and bulk density was determined accounting for

any shrinkage that may have occurred during supercritical fluid extraction (see sample diameters in Table 1). Empirical response surface models were derived from these measurements so that significant effects of the variables on the measured properties could be discerned. Most importantly, the models can be used to predict properties of monoliths prepared using other combinations of polymer and silica and at much lower densities than previously explored.

Within the bounds of the present study, the highest density crosslinked aerogel had the highest stress at failure and exhibited the highest modulus. Stress at failure for these aerogels was 120 times higher than that of the corresponding non-crosslinked aerogels, while density increased only by a factor of three. The lowest density crosslinked aerogels which boasted a nominal density of 0.036 g/cm^3 still exhibited a 15-fold increase in stress at failure over the corresponding uncrosslinked aerogels with a nominal factor of ~1.3 increase in density. Representative stress–strain curves for a higher modulus (run 29) sample and a lower modulus (run 30) sample are provided in Fig. 1, along with the fracture points. Interestingly, the lower modulus sample displays a more gradual fracture under increased strain while the stiffer material fractures completely under maximum stress.

The effects of the three variables, *s*, *d* and *t*, on the measured data were modeled using a full quadratic equation of the form:

$$\text{Property} = A + Bs + Cd + Dt + Es^2 + Fd^2 + Gsd + Hst + Idt \quad (1)$$

where *A* through *I* are coefficients to be derived empirically from experimental data [17]. The model allows terms for first and second order effects of *s* and *d* because experimental runs are included in at least three levels of each of these variables. However, since only two levels of temperature are included in the experimental runs, only the linear effect of *t* can be considered. In addition, the model allows consideration of all three two-way interactive/synergistic terms for *s*, *d* and *t*. All three independent variables were orthogonalized (transformed into a [−1,1] range) prior to modeling, minimizing correlation among terms and responses were log transformed to normalize the data. Terms not deemed statistically significant (<90% confidence) were dropped from the model one at a time by a stepwise modeling technique. Summary statistics (R^2 and standard error) and significant terms in the model are shown in Table 2. For density, all terms were significant in the model. The model for modulus contained all three main effects, a second order effect of *s*, as well as a synergistic effect of silica and temperature (*st*). The model for stress at failure included all three main effects, second order effects of *s* and *d*, as well as a synergistic effect of silane and di-isocyanate concentration (*sd*).

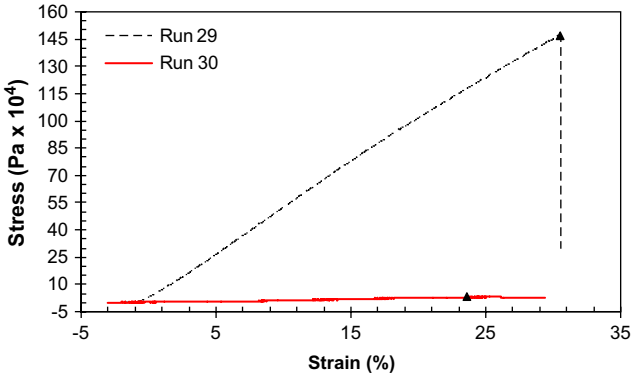

Fig. 1. Representative stress–strain curves showing the range in modulus displayed by aerogels with varied amounts of total silane and polymer crosslinking. Black triangles indicate initial break points.

Graphs of the response surface models for density and maximum stress at failure and modulus are shown in Fig. 2 along with the experimental points. As evidenced from these graphs, increasing silane concentration strongly increases all three measured responses. Density and maximum stress at failure both show an increase with increasing di-isocyanate concentration as well, while the effect on modulus is much less pronounced. For density and maximum stress, the significant synergistic effect between silane and di-isocyanate concentration (*sd*) is also evident. In other words, there is a greater increase in maximum stress with increasing silane concentration when the di-isocyanate concentration is high.

As seen from Fig. 2, temperature also has a pronounced effect on all measured responses. Density, maximum stress and modulus are higher for all combinations of both di-isocyanate and total silane concentration at 71 °C. Also as evidenced by the graphs, the increase in modulus and density is greater at higher di-isocyanate concentrations due to the synergistic effect of *dt*.

Solid ^{13}C CP-MAS NMR spectra as shown in Fig. 3 of selected monoliths reveal approximately twice the amount of polymer incorporated from the 71 °C heated runs compared to those polymerized at room temperature, as evidenced by integrating one of the APTES methylenes (9.5 ppm) against the four methylenes per hexamethylene unit of the di-isocyanate oligomer which appear at 27.5 ppm. These data coupled with a similar increase in density over the uncrosslinked gels, suggest that although at room temperature reaction between the di-isocyanate and the APTES amines on the surface of the silica particles does occur, elevated temperatures facilitate reaction to a greater extent. In addition, chain extension through amines generated *in situ* when water adsorbed on the mesoporous surfaces reacts with the isocyanate moieties is probably also facilitated by higher temperatures [18,19].

While it is clear by observing the response surfaces side by side in Fig. 2 that both maximum stress at failure and modulus increase in concert with increasing density, it is possible to

Table 2
Significant terms and summary statistics for response surface models

Responses	Significant terms	R^2	Standard (RMS) error
Density	*s*, *d*, *t*, s^2, d^2, *sd*, *dt*, *st*	0.98	0.0218 g/cm^2
Stress at failure (log transformed)	*s*, *d*, *t*, s^2, d^2, *sd*	0. 87	0.585
Modulus (log transformed)	*s*, *d*, *t*, s^2, *dt*	0.95	0.489

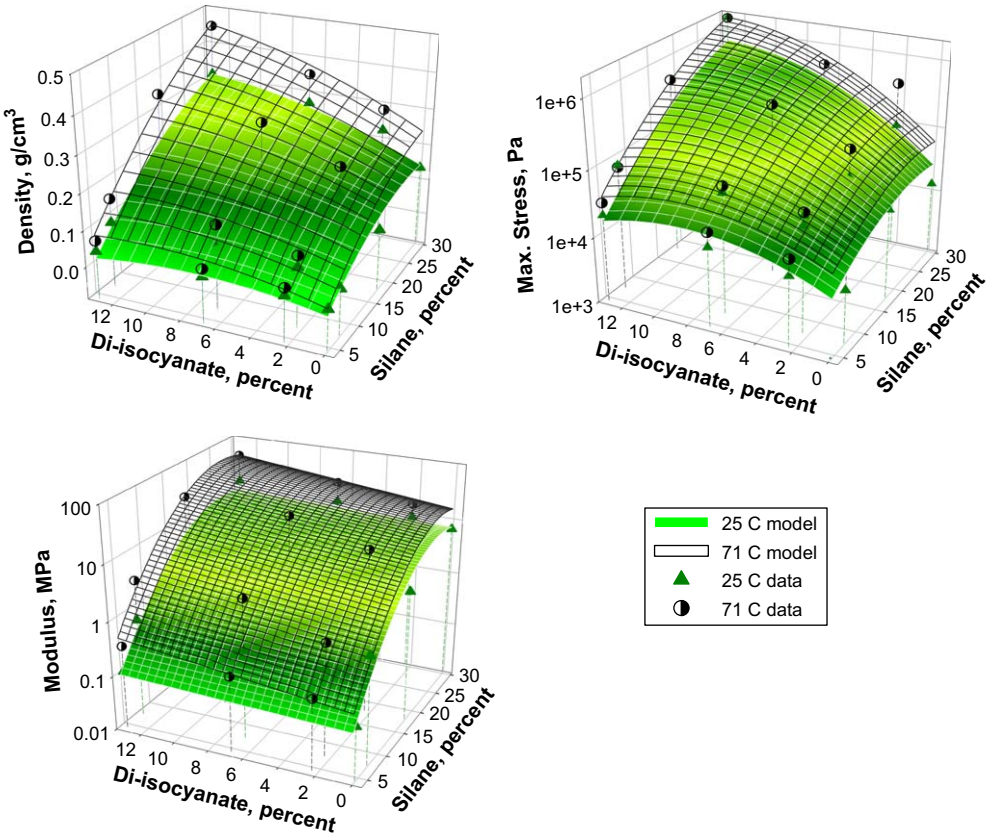

Fig. 2. Response surface models based on data from Table 1 for density, maximum stress at failure and flexural modulus, plotted vs. the di-isocyanate and the total silane (TMOS plus APTES) concentration graphed along with experimental data points.

make monoliths of equal density with very different strengths. To illustrate, in Fig. 4 selective prediction curves from the response surface models are graphed for monoliths with constant initial silane concentration but with different cure temperatures. Of course, the highest maximum stress at failure is ultimately achieved by starting with soaking the highest silane containing gel in the most concentrated di-isocyanate solutions and curing at 71 °C. However, from these curves, it can also be shown that certain room-temperature cured samples, starting with the same initial silane concentration, are predicted to be stronger than their 71 °C cured counterparts of equal density. For example, considering the model generated data points predicted from holding silane concentration constant at 12% (red triangles), a comparison of aerogels at 25 °C (open shapes) and 71 °C (closed shapes) can be made. The increase in density and mechanical properties in these plots are correlated with increasing di-isocyanate solution concentration. The highest density ($\sim$0.15 g/cm^3) monolith made from 12% silica at room temperature is predicted to have a maximum stress at break of 1×10^5 Pa (red dashed arrow). However, a monolith with the same density produced at 71 °C (red solid arrow) is predicted to break at approximately 40% lower stress (6×10^4 Pa). Similarly, with 24% starting silane (blue circles), the highest stress monolith (blue dashed arrow) produced at 25 °C has a density of $\sim$0.26 g/cm^3 and a maximum stress at break of 3×10^5 Pa. The same density monolith produced at 71 °C (blue solid arrow) has a maximum stress of 1.5×10^5 Pa, about half that of the room temperature value.

Monoliths starting with the same amount of silica and having the same final density would have to contain similar amounts of final polymer (noting that the starting di-isocyanate concentration in the solution bath is high for the room temperature cured samples and relatively low for the 71 °C cured samples). Hence, the crosslink tethers produced at the two temperatures must be different in order to explain the difference in strength. The fact that these room-temperature cured samples are stronger than 71 °C cured samples with the same final polymer loading may be because more chain extension takes place in the room temperature samples. If reaction of isocyanate with surface amines is slower at room temperature and there is a large amount of di-isocyanate in the solution, more conversion of isocyanate to amine by adsorbed water would take place. This would result in less but longer polyurea tethers between surface amines at lower temperatures and more resilience even though the weight of polymer incorporated would be similar. At 71 °C, since the reaction of isocyanate with surface amines would be very rapid and the solution of di-isocyanate is at a low concentration, less isocyanate is available to be converted to amine, resulting in more but shorter polyurea tethers.

Curves of modulus vs. density in Fig. 4 show the opposite behavior. In samples with the same resulting bulk density, room temperature cured samples starting with the same initial

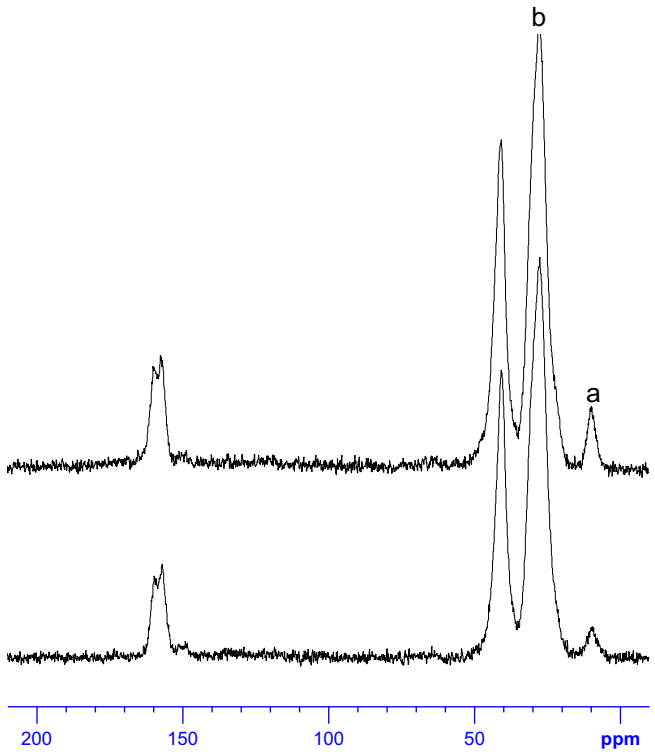

Fig. 3. Solid ^{13}C NMR of di-isocyanate crosslinked aerogel from 17.6% total silane and 2.3% polymer at 25 °C (run 11, top) compared to corresponding monolith prepared at 71 °C (run 14, bottom). Note that peak a at 9.5 ppm is half the size in the bottom spectrum relative to peak b at 27.5 ppm, indicating twice as much incorporation of di-isocyanate at 71 °C.

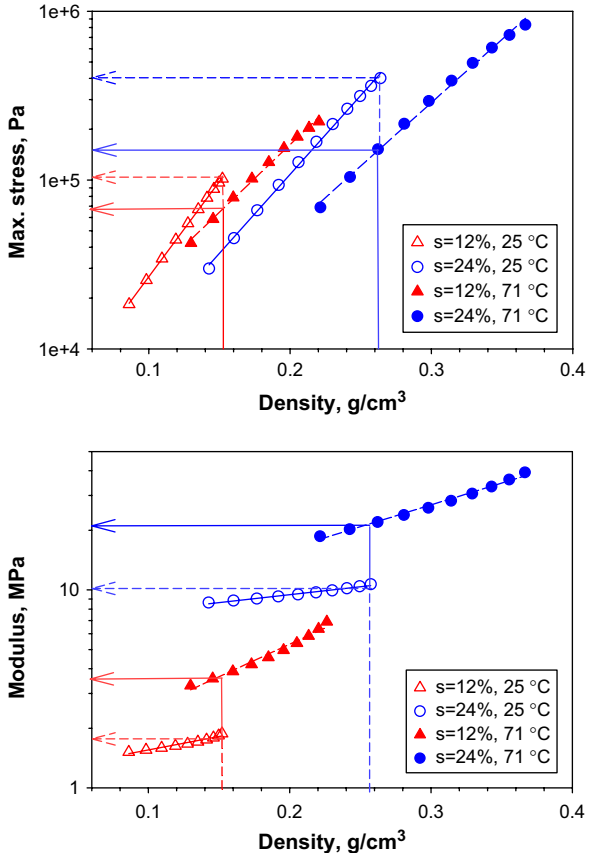

Fig. 4. Predicted plots of maximum stress vs. density (left) and modulus vs. density (right), using model generated data points at 12% (red triangles) and 24% (blue circles) silane concentration. Model generated data show a comparison of aerogels made at 25 °C (open shapes) and 71 °C (closed shapes). The highest stress monolith made from 12% silica at room temperature (10^5 Pa) should have a density ~0.13 g/cm^3. However, a monolith with the same density produced at 71 °C is predicted to break at approximately 40% lower stress. The same is true for all other levels of silica (For interpretation of the references to color in this figure legend, the reader is referred to the web version of this article).

silane concentration are predicted to be of lower modulus than their 71 °C cured counterparts. This observation is also consistent with more crosslinking with amines on the silica surface at 71 °C, resulting in shorter polyurea tethers with higher crosslink density, and hence a stiffer material.

The empirical models can also be used to design an aerogel with a particular set of properties as illustrated in Fig. 5. Slices from the three dimensional surfaces for density and maximum stress cured at 71 °C, and made using no di-isocyanate (red), 6% w/w di-isocyanate (green) and 13% w/w di-isocyanate (blue) are shown (For interpretation of the references to colors, the reader is referred to the web version of this article). As an example, perhaps it is desirable for a particular application to make a polymer crosslinked aerogel with the lowest possible density and a maximum stress at failure of at least 1×10^6 Pa. The point at position A in Fig. 5 shows that this aerogel would have to be made at 71 °C using about 24.5% silane and 13% polymer, and that the density of this aerogel would be a little above 0.4 g/cm^3. If a lower strength could be tolerated (1×10^5 Pa, for example), aerogel B which is made from 7.5% silane and 6% polymer is predicted to have a density of a little over 0.1 g/cm^3. It should also be noted from this figure that the highest strength aerogel achievable within the design space with no polymer crosslinking is approximately 2.5×10^4 Pa – two orders of magnitude lower than the highest polymer crosslinked sample (predicted density as high as 0.15 g/cm^3). Furthermore, this density is nearly identical to that of the di-isocyanate crosslinked aerogel B which is an order of magnitude higher in strength.

To better illustrate how the material's nanostructure relates to the macroscopic properties observed, nitrogen adsorption data were analyzed for surface area and average pore diameter by the Brunauer–Emmet–Teller (BET) method for selected samples from Table 1. Non-crosslinked aerogels from this study typically have a surface area of 600–700 m^2/g depending on the concentration of silanes in the starting sol, while surface areas for the di-isocyanate crosslinked aerogels decrease to a range of 200–300 m^2/g for monoliths crosslinked at 71 °C and 300–400 m^2/g for monoliths crosslinked at room temperature. The average pore diameters [20] follow a similar trend to surface area as non-crosslinked samples have measured pore diameters of around 8.1 nm, while crosslinked samples drop to between 6.4 and 7.5 nm.

Interestingly, as the amount of underlying silica in the polymer crosslinked aerogels is decreased, the monoliths exhibit a change in microstructure. At high densities, as shown in Fig. 6A, the secondary particles resemble a cloud-like

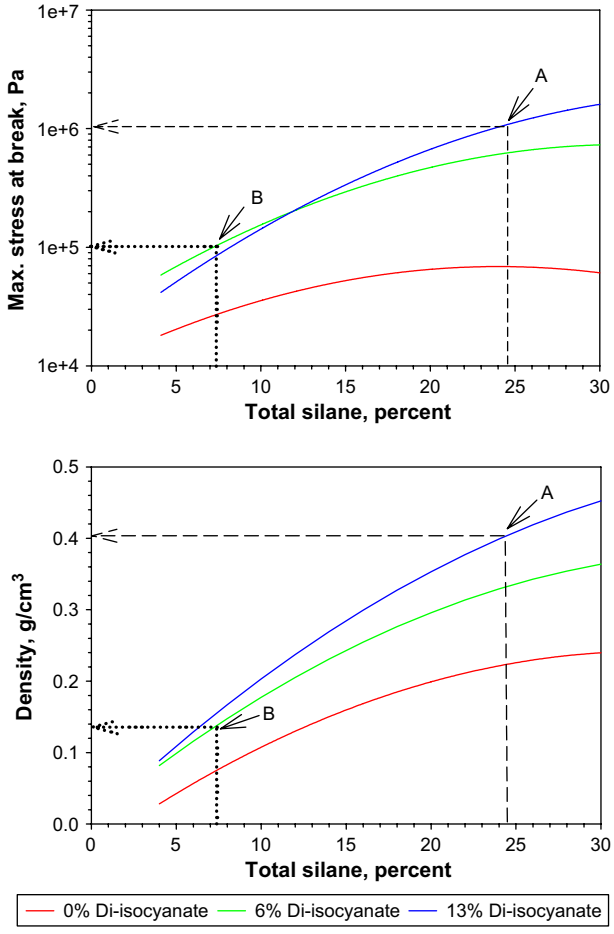

Fig. 5. Slices of the response surface models at 71 °C for maximum stress at break and density plotted vs. total silane concentration.

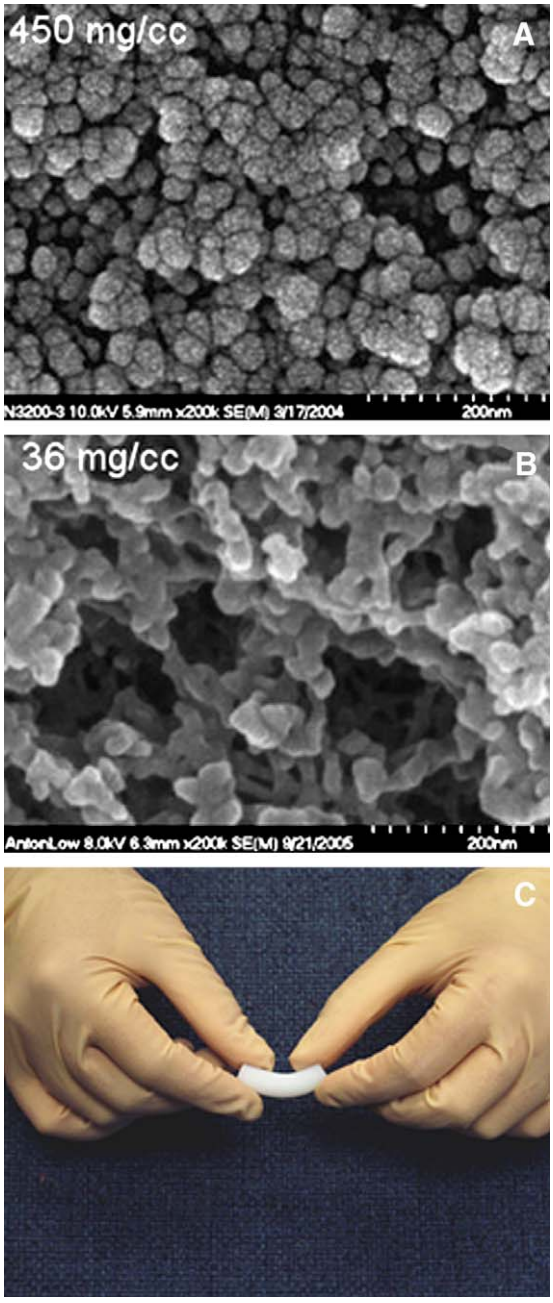

Fig. 6. Comparative microstructure of polymer crosslinked aerogels with higher density (~0.45 g/cm^3) (A) which is relatively inflexible and brittle and lower density (~0.036 g/cm^3) (B) showing change in nanoscale morphology and demonstrating flexibility (C).

configuration with multiple attachments to one another. In contrast, Fig. 6B shows a lower density aerogel with a more fibrous-like, elongated particle arrangement. It also appears that the secondary particles are ill-defined; strongly indicating a thicker polymer coating.

Though the combination of pore diameter and surface area together gives an accurate representation of the material's nanostructure, the true differences in overall nanoporosity are quantified via Eq. (2) where ρ_b is the measured bulk density and ρ_s is the measured skeletal density of the samples.

$$\text{Porosity } \% = \frac{1/\rho_b - 1/\rho_s}{1/\rho_b} \times 100 \qquad (2)$$

Thus, one of the highest density native aerogels produced in this study ($\rho_b = 0.136$ g/cm^3) has a calculated porosity of 91.9%. When this sample was crosslinked using the highest monomer concentration available for this study, the resulting monolith ($\rho_b = 0.312$ g/cm^3) still remains over 75% porous. (To illustrate, consider the dark spaces in Fig. 6A.) In parallel, the porosity of the lowest density native aerogel produced in this study ($\rho_b = 0.026$ g/cm^3) is extremely high (97.5%). When templated with enough polymer to produce the lowest density crosslinked aerogel ($\rho_b = 0.036$ g/cm^3), the monolith retains an astonishing 95.1% empty space (dark spaces in Fig. 6B).

Concomitant with this change in morphology, the monoliths also begin to become flexible. This is demonstrated in Fig. 6C, showing a low-density aerogel monolith (run 27) being flexed to an angle of about 130° without breaking. This property is observed in those crosslinked aerogels with densities less than 0.1 g/cm^3, and is attributed to fewer attachment points between nanoparticles in the lower density nanostructure.

4. Conclusions

Flexibility is a property that aerogels rarely exhibit and thus it is indicative that at very low silica content, the aerogel abandons the properties of the silica template and takes on more properties of the polymer crosslink. Naturally, the use of other types of polymers (toughened epoxies, rubbers, etc.) as crosslinker may introduce even more flexibility into the system. Kramer et al. have demonstrated a similar notion in 1996, with a highly porous ormosil made by supercritically drying a gel made from polydimethyldisiloxane (PDMS) as a co-reactant with TEOS to create an ''aeromosil'' with up to 30% recoverable compressive strain [21].

The notion of utilizing empirical models to tailor aerogels with a particular set of properties for a wide variety of applications can be expanded upon by quantifying a broader range of processing conditions (for example, varying the amount of water, catalyst, washings, reaction time, etc.) for a host of other properties such as thermal conductivity and compressive strength, in addition to density and stress at failure. This is the subject of an expanded study on this family of polymer crosslinked aerogels currently in progress.

Acknowledgements

Financial support from the NASA GRC IR&D Fund, NASA's Low Emission Aircraft Program (LEAP) and Advanced Extravehicular Activities Program (AEVA) is gratefully acknowledged. We also thank Bayer Corporation for providing samples of Desmodur N3200, Ms. Linda McCorkle, Ohio Aerospace Institute for the SEM micrographs, Ms. Anna Palczer for surface analysis and Dr. Amala Dass of the University of Missouri-Rolla for assistance with the three-point flexural bending tests.

References

[1] Morris CA, Anderson ML, Stroud RM, Merzbacher CI, Rolison DR. Science 1999;284:622–4.
[2] Pajonk GM. Catal Today 1999;52:3–13.
[3] Fricke J, Arduini-Schuster MC, Buttner D, Ebert H, Heinemann U, Hetfleisch J, et al. In: Cremers CJ, Fine HA, editors. Thermal conductivity, vol. 21. New York: Plenum Press; 1990. p. 235–45.
[4] Pierre AC, Pajonk GM. Chem Rev 2002;102:4243–65.
[5] Leventis N, Sotiriou-Leventis C, Zhang GH, Rawashdeh AMM. Nano Lett 2002;2:957–60.
[6] Meador MAB, Fabrizio EF, Ilhan F, Dass A, Zhang GH, Vassilaras P, et al. Chem Mater 2005;17:1085–98.
[7] Zhang GH, Dass A, Rawashdeh AMM, Thomas J, Counsil JA, Sotiriou-Leventis C, et al. J Non-Cryst Solids 2004;350:152–64.
[8] Brinker CJ, Scherer GW. Sol–gel science: the physics and chemistry of sol–gel processing. New York: Academic; 1990.
[9] Smith DM, Maskara A, Boes U. J Non-Cryst Solids 1998;225:254–9.
[10] Rettelbach T, Sauberlich J, Korder S, Fricke J. J Non-Cryst Solids 1995;186:278–84.
[11] Iler RK. The chemistry of silica. New York: Wiley; 1979.
[12] Katti A, Shimpi N, Roy S, Lu H, Fabrizio EF, Dass A, et al. Chem Mater 2005;18:285–96.
[13] Husing N, Schubert U, Mezei R, Fratzl P, Riegel B, Kiefer W, et al. Chem Mater 1999;11:451–7.
[14] Husing N, Schubert U. Angew Chem Int Ed 1998;37:22–45.
[15] Tillotson TM, Hrubesh LW. J Non-Cryst Solids 1992;145:44–50.
[16] Sample diameters are shown in Table 1. For samples with densities below $\sim$0.130 g/cm^3, force-deflection data were obtained using a three-point flexural configuration on a TA Instruments Dynamic Mechanical Analyzer (DMA) with a 23 mm span. Due to loading limitations of the DMA, the same force-deflection data were obtained for samples with densities above $\sim$0.130 g/cm^3 with three-point flexural bending following the general guidelines of ASTM D790 using an Instron 4469 test frame also with a 23 mm span.
[17] Statistical modeling was carried out using RS/1 V 6.0.6 and RS/Client for Windows V 2.1.2 from Domain Manufacturing Corporation, Burlington, MA.
[18] Caraculacu AA, Coseri S. Prog Polym Sci 2001;26:799–851.
[19] Two batches of non-APTES containing aerogels were soaked in the same isocyanate solution. One was heated for three days, the other left to react at room temperature. There was negligible polymer uptake in the non-heated gels as the density was increased only very slightly.
[20] Determined by both the $d = 4\ V/A$ method where V is the average pore volume and A is the surface area and the BJH isotherm methods. Both methods yield an average, and were in agreement.
[21] Kramer SJ, Rubio-Alonso F, Mackenzie JD. Mat Res Soc Symp Proc 1996;435:295–300.